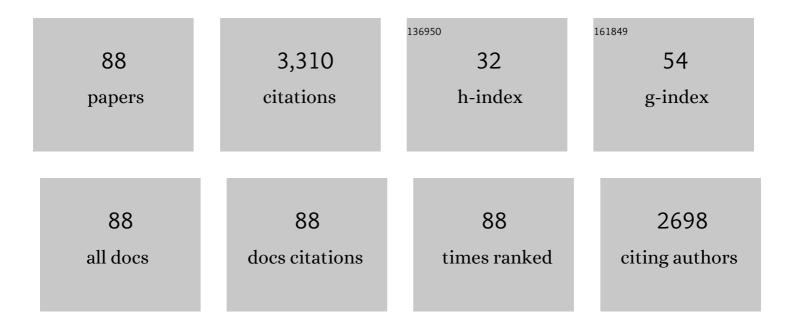
Wenfeng Zhan

List of Publications by Year in descending order

Source: https://exaly.com/author-pdf/1191097/publications.pdf Version: 2024-02-01



#	Article	IF	CITATIONS
1	Strong regulation of daily variations in nighttime surface urban heat islands by meteorological variables across global cities. Environmental Research Letters, 2022, 17, 014049.	5.2	9
2	Urban Heat Islands Significantly Reduced by COVIDâ€19 Lockdown. Geophysical Research Letters, 2022, 49,	4.0	24
3	Longâ€Term and Fineâ€Scale Surface Urban Heat Island Dynamics Revealed by Landsat Data Since the 1980s: A Comparison of Four Megacities in China. Journal of Geophysical Research D: Atmospheres, 2022, 127, .	3.3	4
4	Heat wave-induced augmentation of surface urban heat islands strongly regulated by rural background. Sustainable Cities and Society, 2022, 82, 103874.	10.4	13
5	Identifying analogs of future thermal comfort under multiple projection scenarios in 352 Chinese cities. Sustainable Cities and Society, 2022, 82, 103889.	10.4	4
6	Taxonomy of seasonal and diurnal clear-sky climatology of surface urban heat island dynamics across global cities. ISPRS Journal of Photogrammetry and Remote Sensing, 2022, 187, 14-33.	11.1	23
7	A novel framework to assess all-round performances of spatiotemporal fusion models. Remote Sensing of Environment, 2022, 274, 113002.	11.0	28
8	Diurnally continuous dynamics of surface urban heat island intensities of local climate zones with spatiotemporally enhanced satellite-derived land surface temperatures. Building and Environment, 2022, 218, 109105.	6.9	10
9	A global dataset of spatiotemporally seamless daily mean land surface temperatures: generation, validation, and analysis. Earth System Science Data, 2022, 14, 3091-3113.	9.9	10
10	Meteorological controls on daily variations of nighttime surface urban heat islands. Remote Sensing of Environment, 2021, 253, 112198.	11.0	34
11	Statistical estimation of next-day nighttime surface urban heat islands. ISPRS Journal of Photogrammetry and Remote Sensing, 2021, 176, 182-195.	11.1	12
12	Similarities and disparities in urban local heat islands responsive to regular-, stable-, and counter-urbanization: A case study of Guangzhou, China. Building and Environment, 2021, 199, 107935.	6.9	12
13	Reconciling the inconsistency of annual temperature cycles modelled from Landsat and MODIS LSTs through a percentile approach. International Journal of Remote Sensing, 2021, 42, 7907-7930.	2.9	2
14	Quantification of Urban Heat Island-Induced Contribution to Advance in Spring Phenology: A Case Study in Hangzhou, China. Remote Sensing, 2021, 13, 3684.	4.0	9
15	Reconciling Debates on the Controls on Surface Urban Heat Island Intensity: Effects of Scale and Sampling. Geophysical Research Letters, 2021, 48, e2021GL094485.	4.0	10
16	Assessment of different kernel-driven models for daytime urban thermal radiation directionality simulation. Remote Sensing of Environment, 2021, 263, 112562.	11.0	11
17	A simple yet robust framework to estimate accurate daily mean land surface temperature from thermal observations of tandem polar orbiters. Remote Sensing of Environment, 2021, 264, 112612.	11.0	24
18	Simultaneous investigation of surface and canopy urban heat islands over global cities. ISPRS Journal of Photogrammetry and Remote Sensing, 2021, 181, 67-83.	11.1	47

#	Article	IF	CITATIONS
19	On the land emissivity assumption and Landsat-derived surface urban heat islands: A global analysis. Remote Sensing of Environment, 2021, 265, 112682.	11.0	48
20	Global comparison of diverse scaling factors and regression models for downscaling Landsat-8 thermal data. ISPRS Journal of Photogrammetry and Remote Sensing, 2020, 169, 44-56.	11.1	20
21	Satellite identification of atmospheric-surface-subsurface urban heat islands under clear sky. Remote Sensing of Environment, 2020, 250, 112039.	11.0	21
22	Satellite-based mapping of the Universal Thermal Climate Index over the Yangtze River Delta urban agglomeration. Journal of Cleaner Production, 2020, 277, 123830.	9.3	24
23	A review of earth surface thermal radiation directionality observing and modeling: Historical development, current status and perspectives. Remote Sensing of Environment, 2019, 232, 111304.	11.0	91
24	Analysis of the Spatial and Temporal Variations of Land Surface Temperature Based on Local Climate Zones: A Case Study in Nanjing, China. IEEE Journal of Selected Topics in Applied Earth Observations and Remote Sensing, 2019, 12, 4213-4223.	4.9	32
25	Forecasting of the Nighttime Surface Urban Heat Islands under Clear-sky. , 2019, , .		Ο
26	Seasonal Surface Urban Heat Island Analysis. , 2019, , .		0
27	SUHI analysis using Local Climate Zones—A comparison of 50 cities. Urban Climate, 2019, 28, 100451.	5.7	163
28	Balancing prediction accuracy and generalization ability: A hybrid framework for modelling the annual dynamics of satellite-derived land surface temperatures. ISPRS Journal of Photogrammetry and Remote Sensing, 2019, 151, 189-206.	11.1	45
29	A Method Based on Temporal Component Decomposition for Estimating 1-km All-Weather Land Surface Temperature by Merging Satellite Thermal Infrared and Passive Microwave Observations. IEEE Transactions on Geoscience and Remote Sensing, 2019, 57, 4670-4691.	6.3	97
30	Correction to "A Method Based on Temporal Component Decomposition for Estimating 1-km All-Weather Land Surface Temperature by Merging Satellite Thermal Infrared and Passive Microwave Observations―[Feb 19 4670-4691]. IEEE Transactions on Geoscience and Remote Sensing, 2019, 57, 6254-6254.	6.3	3
31	Assessments of Different Kernel-Driven Models for Modeling Urban Daytime Thermal Anisotropy over Simulation and Satellite Data. , 2019, , .		1
32	Geometric accuracy of remote sensing images over oceans: The use of global offshore platforms. Remote Sensing of Environment, 2019, 222, 244-266.	11.0	25
33	Assessment of offshore oil/gas platform status in the northern Gulf of Mexico using multi-source satellite time-series images. Remote Sensing of Environment, 2018, 208, 63-81.	11.0	32
34	Remote estimation of complete urban surface temperature using only directional radiometric temperatures. Building and Environment, 2018, 135, 224-236.	6.9	24
35	An integrated model for generating hourly Landsat-like land surface temperatures over heterogeneous landscapes. Remote Sensing of Environment, 2018, 206, 403-423.	11.0	94
36	Does quality control matter? Surface urban heat island intensity variations estimated by satellite-derived land surface temperature products. ISPRS Journal of Photogrammetry and Remote Sensing, 2018, 139, 212-227.	11.1	43

#	Article	IF	CITATIONS
37	A geometric model to simulate thermal anisotropy over a sparse urban surface (GUTA-sparse). Remote Sensing of Environment, 2018, 209, 263-274.	11.0	24
38	Identifying industrial heat sources using time-series of the VIIRS Nightfire product with an object-oriented approach. Remote Sensing of Environment, 2018, 204, 347-365.	11.0	62
39	Enhanced Modeling of Annual Temperature Cycles with Temporally Discrete Remotely Sensed Thermal Observations. Remote Sensing, 2018, 10, 650.	4.0	27
40	Identification of typical diurnal patterns for clear-sky climatology of surface urban heat islands. Remote Sensing of Environment, 2018, 217, 203-220.	11.0	80
41	Comprehensive assessment of four-parameter diurnal land surface temperature cycle models under clear-sky. ISPRS Journal of Photogrammetry and Remote Sensing, 2018, 142, 190-204.	11.1	32
42	Variations in satellite-derived carbon dioxide over different regions of China from 2003 to 2011. Atmospheric Environment, 2017, 150, 379-388.	4.1	7
43	A new spectral similarity water index for the estimation of leaf water content from hyperspectral data of leaves. Remote Sensing of Environment, 2017, 196, 13-27.	11.0	39
44	Water use efficiency in response to interannual variations in flux-based photosynthetic onset in temperate deciduous broadleaf forests. Ecological Indicators, 2017, 79, 122-127.	6.3	22
45	Thermal Infrared Contrast Between Different Types of Oil Slicks on Top of Water Bodies. IEEE Geoscience and Remote Sensing Letters, 2017, 14, 1042-1045.	3.1	8
46	A Thermal Sampling Depth Correction Method for Land Surface Temperature Estimation From Satellite Passive Microwave Observation Over Barren Land. IEEE Transactions on Geoscience and Remote Sensing, 2017, 55, 4743-4756.	6.3	58
47	Disaggregation of remotely sensed land surface temperature: A simple yet flexible index (SIFI) to assess method performances. Remote Sensing of Environment, 2017, 200, 206-219.	11.0	9
48	Positive or Negative? Urbanizationâ€Induced Variations in Diurnal Skinâ€Surface Temperature Range Detected Using Satellite Data. Journal of Geophysical Research D: Atmospheres, 2017, 122, 13,229.	3.3	11
49	Spatiotemporal Reconstruction of Land Surface Temperature Derived From FengYun Geostationary Satellite Data. IEEE Journal of Selected Topics in Applied Earth Observations and Remote Sensing, 2017, 10, 4531-4543.	4.9	29
50	Localization or Globalization? Determination of the Optimal Regression Window for Disaggregation of Land Surface Temperature. IEEE Transactions on Geoscience and Remote Sensing, 2017, 55, 477-490.	6.3	18
51	Quantitative Estimation of Carbonate Rock Fraction in Karst Regions Using Field Spectra in 2.0–2.5 μm. Remote Sensing, 2016, 8, 68.	4.0	4
52	Enhanced Statistical Estimation of Air Temperature Incorporating Nighttime Light Data. Remote Sensing, 2016, 8, 656.	4.0	24
53	Quantification of the Scale Effect in Downscaling Remotely Sensed Land Surface Temperature. Remote Sensing, 2016, 8, 975.	4.0	37
54	Detecting and quantifying oil slick thickness by thermal remote sensing: A ground-based experiment. Remote Sensing of Environment, 2016, 181, 207-217.	11.0	62

#	Article	IF	CITATIONS
55	Disaggregation of remotely sensed land surface temperature: A new dynamic methodology. Journal of Geophysical Research D: Atmospheres, 2016, 121, 10,538.	3.3	32
56	Surface urban heat island effect and its relationship with urban expansion in Nanjing, China. Journal of Applied Remote Sensing, 2016, 10, 026037.	1.3	40
57	Temporal upscaling of surface urban heat island by incorporating an annual temperature cycle model: A tale of two cities. Remote Sensing of Environment, 2016, 186, 1-12.	11.0	66
58	Satellite data lift the veil on offshore platforms in the South China Sea. Scientific Reports, 2016, 6, 33623.	3.3	12
59	Time series decomposition of remotely sensed land surface temperature and investigation of trends and seasonal variations in surface urban heat islands. Journal of Geophysical Research D: Atmospheres, 2016, 121, 2638-2657.	3.3	86
60	Automatic extraction of offshore platforms using time-series Landsat-8 Operational Land Imager data. Remote Sensing of Environment, 2016, 175, 73-91.	11.0	37
61	Retrieval of three-dimensional tree canopy and shade using terrestrial laser scanning (TLS) data to analyze the cooling effect of vegetation. Agricultural and Forest Meteorology, 2016, 217, 22-34.	4.8	95
62	Automated extraction of tidal creeks from airborne laser altimetry data. Journal of Hydrology, 2015, 527, 1006-1020.	5.4	21
63	Forest aboveground biomass estimation using polarization coherence tomography and PolSAR segmentation. International Journal of Remote Sensing, 2015, 36, 530-550.	2.9	12
64	Landsat 8 OLI image based terrestrial water extraction from heterogeneous backgrounds using a reflectance homogenization approach. Remote Sensing of Environment, 2015, 171, 14-32.	11.0	123
65	Comparing surface- and canopy-layer urban heat islands over Beijing using MODIS data. International Journal of Remote Sensing, 2015, 36, 5448-5465.	2.9	48
66	An elevation difference model for building height extraction from stereo-image-derived DSMs. International Journal of Remote Sensing, 2014, 35, 7614-7630.	2.9	22
67	Disaggregation of Remotely Sensed Land Surface Temperature: A Generalized Paradigm. IEEE Transactions on Geoscience and Remote Sensing, 2014, 52, 5952-5965.	6.3	31
68	Satellite-Derived Subsurface Urban Heat Island. Environmental Science & Technology, 2014, 48, 12134-12140.	10.0	36
69	Estimating mean air temperature using MODIS day and night land surface temperatures. Theoretical and Applied Climatology, 2014, 118, 81-92.	2.8	31
70	Remotely sensed soil temperatures beneath snow-free skin-surface using thermal observations from tandem polar-orbiting satellites: An analytical three-time-scale model. Remote Sensing of Environment, 2014, 143, 1-14.	11.0	45
71	A hybrid method combining neighborhood information from satellite data with modeled diurnal temperature cycles over consecutive days. Remote Sensing of Environment, 2014, 155, 257-274.	11.0	39
72	A simple error estimation method for linear-regression-based thermal sharpening techniques with the consideration of scale difference. Geo-Spatial Information Science, 2014, 17, 54-59.	5.3	10

#	Article	IF	CITATIONS
73	Improved reconstruction of soil thermal field using two-depth measurements of soil temperature. Journal of Hydrology, 2014, 519, 711-719.	5.4	24
74	Multi-temporal trajectory of the urban heat island centroid in Beijing, China based on a Gaussian volume model. Remote Sensing of Environment, 2014, 149, 33-46.	11.0	143
75	A generic framework for modeling diurnal land surface temperatures with remotely sensed thermal observations under clear sky. Remote Sensing of Environment, 2014, 150, 140-151.	11.0	26
76	Land Surface Temperature Retrieval from MODIS Data by Integrating Regression Models and the Genetic Algorithm in an Arid Region. Remote Sensing, 2014, 6, 5344-5367.	4.0	22
77	Disaggregation of remotely sensed land surface temperature: Literature survey, taxonomy, issues, and caveats. Remote Sensing of Environment, 2013, 131, 119-139.	11.0	269
78	Modelling the diurnal variations of urban heat islands with multi-source satellite data. International Journal of Remote Sensing, 2013, 34, 7568-7588.	2.9	83
79	DEM Densification Using Perspective Shape From Shading Through Multispectral Imagery. IEEE Geoscience and Remote Sensing Letters, 2013, 10, 145-149.	3.1	12
80	Intercomparison of methods for estimating land surface temperature from a Landsat-5 TM image in an arid region with low water vapour in the atmosphere. International Journal of Remote Sensing, 2012, 33, 2582-2602.	2.9	47
81	Assessment of thermal anisotropy on remote estimation of urban thermal inertia. Remote Sensing of Environment, 2012, 123, 12-24.	11.0	33
82	Downscaling land surface temperatures with multi-spectral and multi-resolution images. International Journal of Applied Earth Observation and Geoinformation, 2012, 18, 23-36.	2.8	44
83	Interpolating diurnal surface temperatures of an urban facet using sporadic thermal observations. Building and Environment, 2012, 57, 239-252.	6.9	21
84	A modified single-channel algorithm for land surface temperature retrieval from HJ-1B satellite data. Hongwai Yu Haomibo Xuebao/Journal of Infrared and Millimeter Waves, 2012, 30, 61-67.	0.2	12
85	Maximum Nighttime Urban Heat Island (UHI) Intensity Simulation by Integrating Remotely Sensed Data and Meteorological Observations. IEEE Journal of Selected Topics in Applied Earth Observations and Remote Sensing, 2011, 4, 138-146.	4.9	78
86	Sharpening Thermal Imageries: A Generalized Theoretical Framework From an Assimilation Perspective. IEEE Transactions on Geoscience and Remote Sensing, 2011, 49, 773-789.	6.3	69
87	An Algorithm for Separating Soil and Vegetation Temperatures With Sensors Featuring a Single Thermal Channel. IEEE Transactions on Geoscience and Remote Sensing, 2011, 49, 1796-1809.	6.3	20
88	Improvement of mono-window algorithm for retrieving land surface temperature from HJ-1B satellite data. Chinese Geographical Science, 2010, 20, 123-131.	3.0	19